S20-33

50448

125134

Development of a Hermetically Sealed Brushless DC Motor for a J-T Cryocooler

Edwin Joscelyn*, Irwin Hochler*, Andrew Ferri*, Heinz Rott*, and Ted Soukaris*

Abstract

This development was sponsored by Ball Aerospace for the Cryogenic On-Orbit Long-Life Active Refrigerator (COOLLAR) program. The cryocooler is designed to cool objects to 65° K and operate in space for at least 7 years. The system also imports minimal impact to the spacecraft in terms of vibration and heat.

The basic Joule-Thompson cycle involves compressing a working fluid, nitrogen in this case, at near-constant temperature from 17.2 KPa to 6.89 MPa. The nitrogen is then expanded through a Joule-Thompson valve. The pure nitrogen gas must be kept clean; therefore, any contamination from motor organic materials must be eliminated. This requirement drove the design towards sealing of the motor within a titanium housing without sacrificing motor performance. It is estimated that an unsealed motor would have contributed 1.65 g of contaminants, due to the organic insulation and potting materials, over the 7-year life. This paper describes the motor electrical and mechanical design, as well as the sealing difficulties encountered, along with their solutions.

Introduction

The COOLLAR drive system consists of a motor, tachometer, synchro, and the drive electronics. Aeroflex's responsibility was for the motor design and the synchro integration. The other components were supplied by Ball Aerospace. A photograph of the motor and synchro assembly together with the rotor is shown in Figure 1.

The motor is a three-phase permanent magnet torque motor, which is driven by a sinusoidal current source. The current source is derived from the system synchro. In order to meet the allowable inertial disturbances generated by the drive system, the torque ripple spectrum under all operating conditions should be within the limits shown in Figure 2. The disturbance torques are generated by the harmonics of the motor torque constants and the synchro outputs, and by slot lock. The commutation torque ripple is zero if the motor torque constants and the synchro outputs are mathematical sine waves; therefore, to maintain the commutation ripple within acceptable levels, the harmonics have to be carefully controlled. The slot lock torque ripple is minimized by the slot/pole combination and rotor skewing. The motor operates at 12.5 to 44 rad/s at a torque load up to approximately 10.6 N-m. The specification for the motor is as follows:

* Aeroflex Laboratories Inc., Farmingdale, New York

Kt_{phase}.......... 76 (+/- 4) N-m/amp
R_{Phase} .... 0.151 (± 0.014) ohms
Poles 16
Phases ..... 3 (not interconnected, open delta)
O.D. .... 0.177 m maximum
Length .... 0.081 m

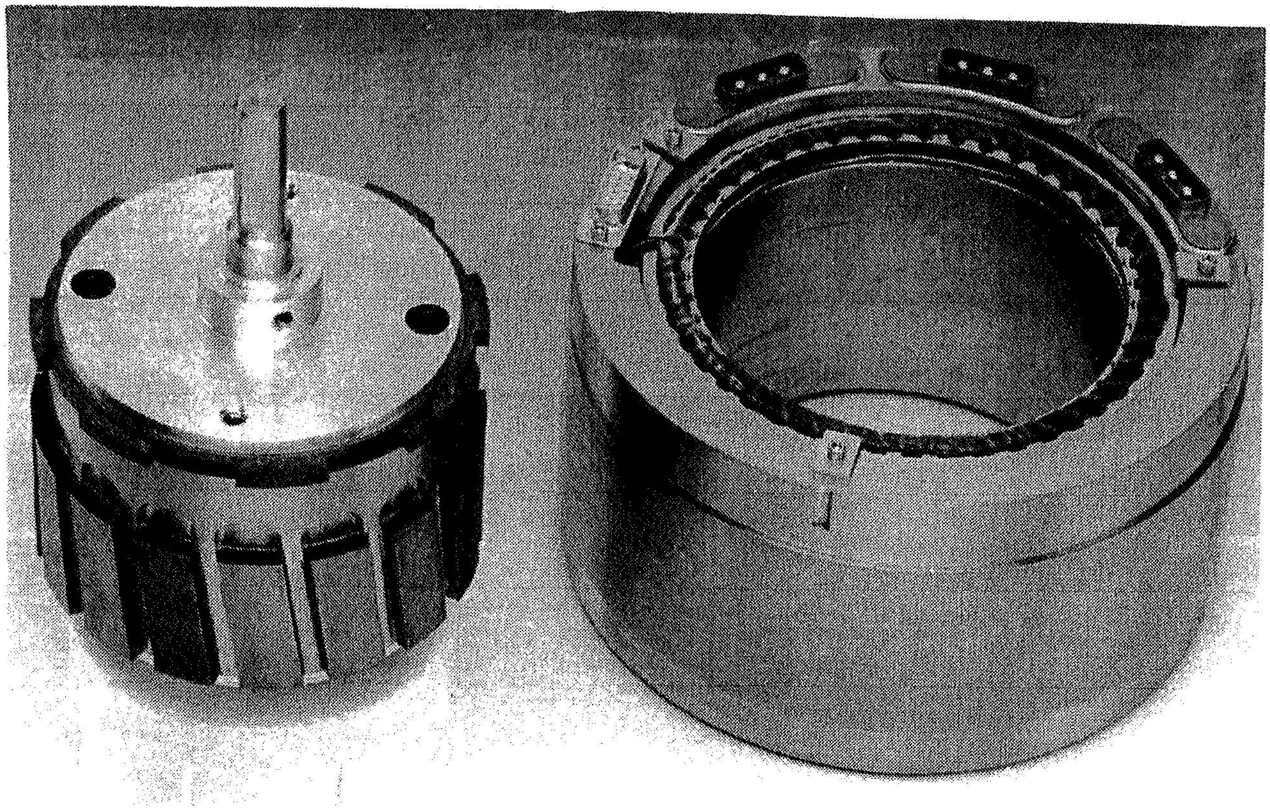

Figure 1 Motor/Synchro Photograph

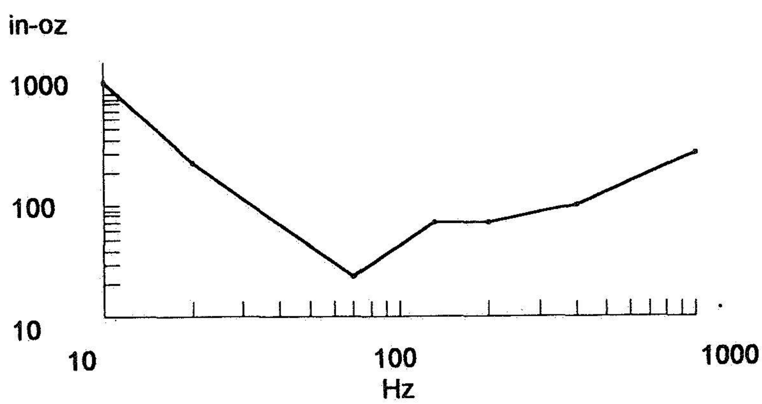

Figure 2 Allowable Torque Ripple Spectrum

Motor Design

There are a variety of slot/pole configurations which will give a sinusoidal back EMF waveform (and therefore a sinusoidal K_t). A convenient arrangement, as shown by Hendershot [1], is a 2.25 slot/pole ratio with a 15° pole angle for a 16-pole skewed rotor. The stator has 36 slots.

The first order of business was to determine the torque capability of this configuration for the physical size allowed. Finite Element Analysis (FEA) was used to determine the flux density in the air gap so that conventional Lorentz force calculations could be made. The FEA technique also allows the rotor to be displaced by a small angle where the change in energy is used to calculate torque using the principle of virtual work.

The maximum length that the physical constraints allow is a stack of 0.043 m. The maximum diameter of the rotor is 0.113 m. The physical air gap is 0.41 mm, and the magnetic air gap is 0.66 mm, which allows room for the titanium shell which seals the motor from the nitrogen. An FEA equipotential line plot, generated by the magnets with a single phase winding excited, is shown in Figure 3.

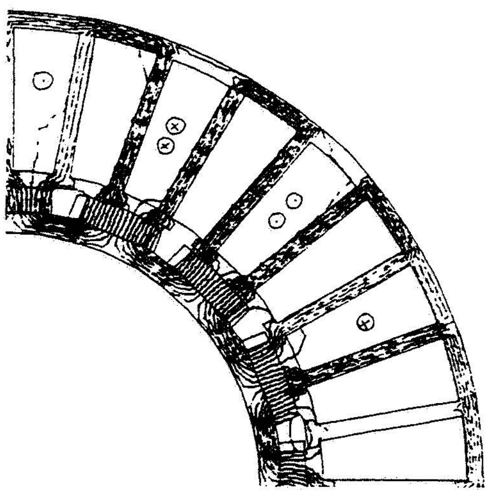

Figure 3 Magnetic FEA Model

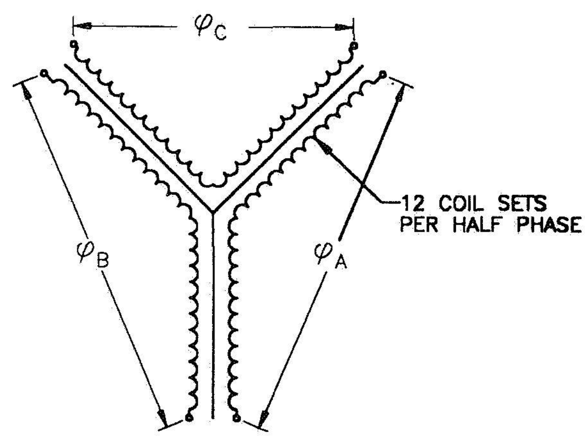

Figure 4 Winding Diagram

From the FEA, the resultant flux density in the air gap is 1.05 W/m^2. In order to affect an unconnected winding, yet preserve the sinusoidal waveform given by a wye winding, the motor was wound as shown in Figure 4.

Each of the 24 coils which form a single phase has 6 turns of wire. This gives an effective length of 12.7 m per phase. This calculates to a K_t of 0.362 N-m/amp for 1/2 phase, using the Lorentz method. For a sinusoidal waveform, the K_t for a leg-to-leg winding (making 1 phase in our winding scheme) is 1.5 times the 1/2 phase value, or 0.54 N-m/amp. Subtracting a 6% loss due to a 1 slot skew gives a 0.51 N-m/amp torque constant prediction.

Using FEA to generate a predicted torque constant via the virtual work principle, the rotor was displaced 2° with the change in energy divided by the angle yielding torque. The FEA results for this model is 0.050 Joules/0.0349 radians = 1.43 N-m. Multiplying by 4, since only 1/4 of the model is analyzed, and dividing by the 10 A used in the analysis gives a K_t = 0.57 N-m/amp. Skewing reduces K_t to 0.536 N-m/amp. Both of these predictions, 0.511 N-m/amp and 0.536 N-m/amp were close, since the actual performance result was 0.515 N-m/amp. The motor resistance was 0.143 ohms.

Mechanical Considerations

The system design requires that the motor be a "plug-in" unit (i.e. the specially designed hermetic connectors need precise alignment with the housing outer dimensions). This, in turn, requires that the lamination stack be dimensionally concentric to locate centrally within the titanium housing. The lamination material is vanadium permendur because the winding area had to be maximized, due to the densely packed 32-filar winding needed to achieve the required low resistance. Lamination manufacturers were not willing to hold the tolerances required to allow precise stacking after heat treatment because this metal tends to buckle and move. This problem was solved by laminating heat-treated sheets to the 0.043-m dimension and using EDM techniques to cut the finished lamination stack. The edges were remarkably clean with the dimensions precise to 0.025-mm tolerances.

The next problem was the titanium shell design. It was recognized that attempting to machine the inner diameter to 0.254 mm thick would have been a problem. Either the extremely thin part would wrinkle during machining, or the wall could distort due to the insertion and bonding of the stator. Another concern was where to make the seams for electron beam welding of the final seal. The approach was to pre-machine the inner diameter with a thick wall, install and bond the stator, and machine the inner diameter to the thin wall required. Figure 5 shows a cross-section diagram of the motor. The seam to be electron beam welded is indicated.

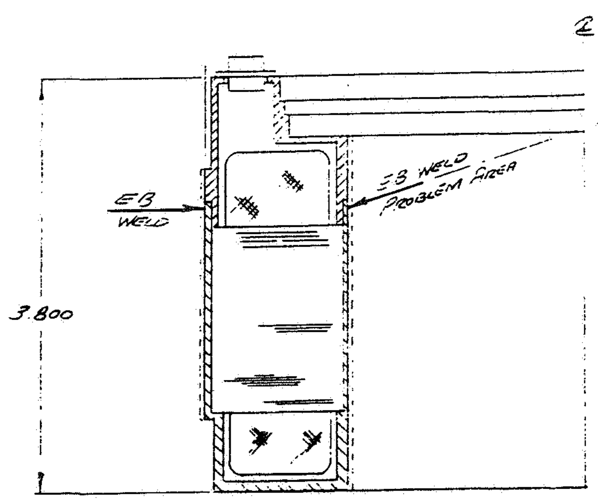

Figure 5 Initial Seam Configuration

Electron Beam Welding

Titanium is particularly well-suited for electron beam welding. Initial attempts at welding, however, were disastrous. The weld was difficult for the welder to approach from the inside, and the material burned through, thus leaving holes in the seam. The beam could not burn through to the appropriate depth without melting excessive surrounding material which, in turn, caused the holes. Even though earlier test sections, which were flat representations of the overlapping interface, were successfully welded, it became obvious, after several attempts, that the design approach needed to be changed. The new approach is reflected in Figure 6.

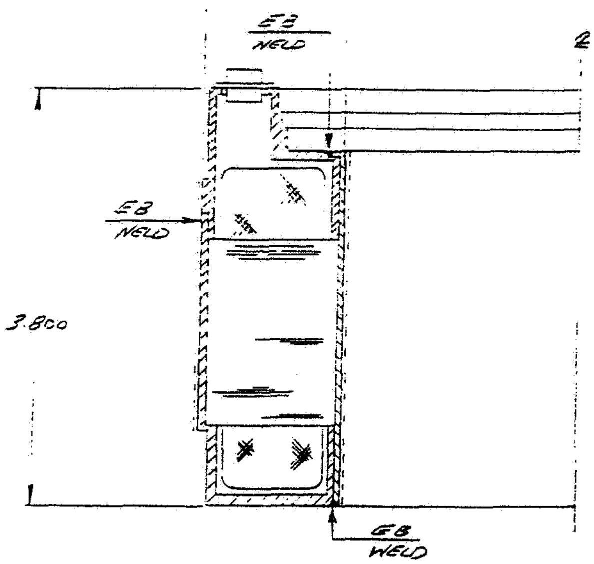

Figure 6 Final Seam Configuration

This approach eliminated the thin-wall sections where the weld was to occur. This design allowed easy access to the welder, and the thicker cross-sections allowed the beam to penetrate and weld properly. The inner cylinder was still initially pre-machined with a thicker cross-section and machined after welding.

The connector design was a custom hermetic seal with three pins for each phase (one for case ground). The connectors were fixed relative to the outer diameter for the "plug-in" interface and electron beam welded to the top of the motor. Because of the flat, thick surface, electron beam welding was not a problem in this area

Motor Losses Due to the Titanium

A concern is the magnitude of eddy current losses due to the titanium. Eddy currents are proportional to the magnetic frequency squared, the length of the eddy current path squared, the flux density squared, and the material volume. The eddy currents are inversely proportional to the material resistivity. Calculating the power [2]:

$$P_{eddy} = \pi^2 f^2 \tau^2 \beta^2 \, \upsilon / 6\rho$$

where (all MKS units) f is the magnetic reversal frequency, τ is the stack length, β is the flux density, υ is the volume of titanium, and ρ is the resistivity for the motor rotating at 40 rad/s, gives a power loss of 17.3 watts. The flux distribution in the material is sinusoidal and does not cover the entire volume at all times with maximum value. More appropriately, the value above is reduced by the 75% magnet coverage and the average for a squared sine wave, which is 0.5. This gives a theoretical power loss of 6.4 watts.

The actual power loss was measured by taking the difference between the motor drag torque at 40 rad/s housed and unhoused. The power loss due to the 0.254-mm layer of titanium was measured as 6 watts.

Conclusions

"Clean" motors can be manufactured in this manner. The losses were only 1.4% of the peak operating power for this motor. Smaller motors operating at faster speeds can be made with thinner internal wall thicknesses. Applications that require motors placed near optical elements would be natural for this technology. Step motors which place objects in and out of optical paths, such as filter wheels, would also benefit from this approach. The COOLLAR drive system has been tested at Ball Aerospace with superlative performance results.

References

1. Hendershot, J.R. "Design of Brushless Permanent-Magnet Motors." Magna Physics Corp., Publishing Division, (1990), pp103.

2. E.E. Staff, MIT. "Magnetic Circuits and Transformers." John Wiley (1943), pp136-137.